

# Advanced Techniques for Spectrally Efficient DVB-S2X Systems

Alessandro Ugolini\*, Andrea Modenini\*, Giulio Colavolpe\*, Giorgio Picchi\*, Vittoria Mignone<sup>†</sup>, Alberto Morello<sup>†</sup>

\*DII, University of Parma, Italy, email: {alessandro.ugolini, andrea.modenini, giulio, giorgio.picchi}@unipr.it

<sup>†</sup>Research and Technology Innovation Centre, RAI, Torino, Italy, email: {vittoria.mignone, alberto.morello}@rai.it

**Abstract**—We investigate different techniques to improve the spectral efficiency of systems based on the DVB-S2 standard, when the transmitted signal bandwidth cannot be increased because it has already been optimized to the maximum value allowed by transponder filters. We will investigate and compare several techniques to involve different sections of the transceiver scheme. The techniques that will be considered include the use of advanced detection algorithms, the adoption of time packing, and the optimization of the constellation and shaping pulses. The LDPC codes recently proposed for the evolution of the DVB-S2 standard will be considered, as well as the adoption of iterative detection and decoding. Information theoretical analysis will be followed by the study of practical modulation and coding schemes.

## I. INTRODUCTION

In recent years, the need to satisfy the growing demand for high data rates pushed the investigation towards the development of many techniques aimed at increasing the spectral efficiency (SE) of satellite systems. The second-generation specification of the digital video broadcasting for satellite (DVB-S2) [1] was developed in 2003 with the main aim of improving the system performance with a reasonable receiver complexity. At the end of 2012, the DVB project has initiated the development of an evolution of DVB-S2, which was approved by DVB in March 2014 with the name of DVB-S2X and will be published as Part II of ETSI Standard EN 302307 [2].

Common DVB-S2 transmitters use baudrates of approximately 30 Mbaud and shaping pulses with a root-raised cosine (RRC) spectrum with roll-off factors greater than or equal to 0.2. These relatively high roll-off values make easy the implementation of shaping filters and timing recovery, while the baudrate values have been chosen to guarantee low interference from adjacent transponders and to ensure that on-board satellite equipment is able to cope with the power dissipated by transponder filters [3]. At the receiver, symbol-by-symbol detection is usually performed, followed by the decoding stage.

However, nowadays technological evolution allows to adopt smaller roll-off factors and more sophisticated detection/decoding techniques. As a consequence, it has been recently considered to increase the baudrate of DVB-S2 signals despite this could involve a complexity increase. The target of the analysis performed in [3] was to compare the SE for two different detection schemes with different complexity

(still based on symbol-by-symbol detection after, possibly, the adoption of a proper linear equalizer) for several baudrate and roll-off values: the suggested combination resulted in a system with baudrates of 36~37 Mbaud, RRC pulses with roll-off 0.1, static data predistortion at the transmitter and the use of a fractionally-spaced equalizer at the receiver. Higher baudrate values have been discarded, since they would cause problems related to power dissipation and to interchannel interference. It is important to remark that the presence of an equalizer allows the system to better handle the increased distortions and interference arising when working with higher baudrate values.

In light of these considerations, the investigation reported in this paper is aimed at improving the performance of the best system described in [3], that will be considered as the starting point. Since we are constrained to work with a baudrate not greater than 37 Mbaud (corresponding to a bandwidth of 40.7 MHz when pulses with roll-off 0.1 are used) the candidate solutions, that will be considered throughout the paper are the following.

*The use of a more sophisticated detection algorithm.* It is reasonable to think that the use of a highly performing detector, specifically tailored for the nonlinear satellite channel, could increase the SE values.

*The use of new channel codes.* New codes, having a better design and higher granularity than those foreseen by the DVB-S2 standard, could improve performance.

*The application of faster-than-Nyquist or time packing.* It has been shown for several scenarios that the SE can be increased by giving up the orthogonality condition at the transmitter, thus intentionally introducing intersymbol interference (ISI) [4]–[10]. This could also be achieved by properly increasing the signal bandwidth at the transmitter output as shown in [10], where a roll-off equal to 0.2 is assumed for the RRC shaping pulses. For fixed transponder filter bandwidths, an increase of the signal bandwidth will result in an increase of ISI. Since, as mentioned, the signal bandwidth cannot be larger than approximately 40 MHz, a further bandwidth increase is not feasible; however, the use of time packing adds another degree of freedom that can be properly exploited.

*The optimization of the transmitted pulse and/or the constellations.* The shaping pulse and/or the constellation can be properly designed in order to maximize the SE.

These techniques can also be combined. As an example,

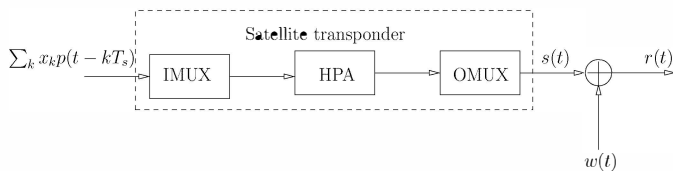


Figure 1. Block diagram of the satellite transponder.

time packing can take advantage of the use of more sophisticated detection algorithms able to cope with the introduced (linear and nonlinear) ISI or of the use of a properly designed shaping pulse or constellation. Thus, separate investigations of these techniques would lead to wrong conclusions and an incomplete investigation. In case these techniques provide an improvement in terms of SE, it is not guaranteed that the same gain can be achieved by using the modulation and coding formats (MODCODs) already adopted in DVB-S2 standard or in its extension DVB-S2X [2]—a design of new specifically tailored codes could be required.

The remainder of this paper is structured as follows. Section II describes the system model adopted throughout the paper, Section III introduces the figures of merit we have used to evaluate the performance of the studied systems. Section IV presents some detection algorithms specifically designed for the nonlinear satellite channel. Sections V and VI describe some advanced techniques to improve the spectral efficiency. Section VII discusses the numerical results for all described techniques and, finally, some conclusions are drawn in Section VIII.

## II. SYSTEM MODEL

We consider a single-carrier-per-transponder scenario, where each satellite transponder is assumed to work with a single carrier occupying the entire transponder bandwidth. In this case, the on-board power amplifier can operate closer to saturation and hence improve its efficiency.

The complex envelope of the signal transmitted over the carrier under consideration can be expressed as

$$\sum_{k=0}^{K-1} x_k p(t - kT_s),$$

where  $\{x_k\}_{k=0}^{K-1}$  are the  $K$  transmitted symbols. The base pulse  $p(t)$  has RRC shaped spectrum with roll-off factor  $\alpha$ , and the symbol interval is  $T_s = \tau T$ , where  $T$  is half of the main lobe duration and  $\tau \leq 1$  is a compression factor to be better specified later. The signal bandwidth, constrained to be limited to approximately 40 MHz, is  $W = (1 + \alpha)/T$ . The transmitted symbols belong to a given zero-mean complex constellation  $\mathcal{C}$  having cardinality  $|\mathcal{C}| = M$ , possibly predistorted [11]. We will consider these  $M$ -ary symbols as obtained from binary encoded symbols (possibly interleaved) through a proper mapping.

The block diagram of the satellite transponder is shown in Figure 1. It includes an input multiplexer (IMUX) filter

which removes the adjacent channels, a high power amplifier (HPA), and an output multiplexer (OMUX) filter aimed at reducing the spectral broadening caused by the nonlinear amplifier. The HPA AM/AM and AM/PM characteristics and the IMUX/OMUX impulse responses are perfectly known at the transmitter and at the receiver and are described in [1], and the OMUX filter has -3 dB bandwidth equal to 38 MHz. Although the HPA is a nonlinear memoryless device, the overall system has memory due to the presence of IMUX and OMUX filters.

The received signal is further corrupted by additive white Gaussian noise (AWGN) whose low-pass equivalent  $w(t)$  has power spectral density  $2N_0$ . The received signal can be expressed as

$$r(t) = s(t) + w(t),$$

where  $s(t)$  is the signal at the output of the transponder.

## III. FIGURES OF MERIT

This section introduces the different figures of merit used to assess the performance of the considered systems and techniques. The most important one is represented by the *spectral efficiency* (SE) that can be achieved by a given MODCOD. It is defined as

$$SE = \frac{r \log_2(M)}{T_s B_{\text{OMUX}}},$$

where  $B_{\text{OMUX}} = 38$  MHz is the -3 dB bandwidth of the OMUX filter [1], and  $r$  is the rate of the adopted code. We point out that other bandwidth definitions could be used as reference without any loss of generality and any modification in the conclusions. The SE that can be achieved by a given MODCOD is often represented into the Shannon plane as a function of  $P_{\text{sat}}/N$ ,  $P_{\text{sat}}$  being the HPA power at saturation and  $N$  the noise power, corresponding to a target packet error rate (PER) of  $10^{-3}$ .

We will also consider an information-theoretic figure of merit represented by the *achievable spectral efficiency* (ASE), whose definition is

$$ASE = \frac{I_R}{T_s B_{\text{OMUX}}}, \quad (1)$$

being  $I_R$  the *achievable information rate* that, for a system with memory, can be computed by means of the Monte Carlo method described in [12]. When a suboptimal detector is employed, this technique gives an achievable lower bound on the actual information rate, corresponding to the information rate of the considered channel when that suboptimal detector is adopted [13]. The ASE for a given transceiver scheme (modulation, shaping pulse, baudrate and detector) shows the maximum SE that can be achieved by any practical MODCOD and employing joint detection and decoding. It can thus be computed with no reference to a practical coding scheme [12].

Finally, we will also consider the pragmatic ASE (p-ASE) defined as in (1), but with  $I_R$  substituted by the *pragmatic information rate* (also known as *BCJR-Once Rate* [14]). The p-ASE represents an upper bound on the SE of practical

MODCODs, when detection and decoding are performed separately, without any iteration between them.

#### IV. DETECTION ALGORITHMS FOR THE NONLINEAR SATELLITE CHANNEL

In this section, we describe some detection algorithms, specifically designed for the nonlinear satellite channel. We will consider the optimal maximum a posteriori (MAP) detection and lower complexity alternatives.

##### A. Optimal MAP Detection for the Satellite Channel: the Chip Detector

The nonlinear transponder and the possible application of the time packing technique (to be detailed later) introduce (nonlinear) ISI on the transmitted signal. Assuming that the system is finite-memory, we can model the modulator, IMUX and OMUX filters, and the HPA as a finite-state machine (FSM), whose input is the symbol sequence  $\{x_k\}_{k=0}^{K-1}$  and whose output is the signal

$$s(t) = \sum_{k=0}^{K-1} \bar{s}(t - kT_s, x_k, \sigma_k),$$

where signal  $\bar{s}(t - kT_s, x_k, \sigma_k)$  is assumed to have support in the interval  $[kT_s, (k+1)T_s)$  and is thus a “chip” (a slice) of the signal. The state  $\sigma_k$  of the FSM contains the previous  $L$  channel inputs,  $L$  being the memory length of the channel

$$\sigma_k = (x_{k-1}, x_{k-2}, \dots, x_{k-L}).$$

Therefore, the optimal MAP symbol detector consists of a bank of filters [15] matched to all possible waveforms  $\bar{s}(t - kT_s, x_k, \sigma_k)$ , followed by a Bahl-Cocke-Jelinek-Raviv (BCJR) detector [16]. The complexity of the BCJR algorithm is  $\mathcal{O}(M^{L+1})$ . In principle, the real channel memory can be much larger than that assumed by the detection algorithm—the choice of  $L$  is often dictated by implementation complexity reasons, thus resulting in a suboptimal implementation. The chip detector can be also used jointly with a predistorter at the transmitter.

##### B. Lower Complexity Detection Algorithms

The chip detector tends to be optimal for  $L \rightarrow \infty$ , independently of the HPA, IMUX, and OMUX characteristics and of the possible application of the time packing technique. However, its complexity for optimal detection becomes soon unmanageable unless proper techniques for complexity reduction are employed. For the sake of clarity, let us just consider, for example, the case of transmission of a linear modulation with orthogonal signaling on the AWGN channel. It is known that, in this case, the symbol-by-symbol detector is optimal. On the other hand, the chip detector would require a large memory  $L$ , since it does not exploit the linear nature of the received signal and the orthogonality condition. In light of these considerations, it is reasonable to think that the optimal performance achieved by the chip detector may be reached by lower complexity algorithms, using smaller values of  $L$ . For this reason, we found it convenient to consider other detection algorithms beyond the chip detector.

*SISO detection based on Volterra model:* A soft-input soft-output (SISO) detection algorithm for the nonlinear satellite channel has been proposed in [17] based on the relevant terms of the Volterra series expansion of the nonlinear HPA proposed in [18]. It is composed of a suitably designed filter, followed by a BCJR algorithm with proper branch metrics, taking into account only a portion  $L$  of the actual channel memory.

*FS-MMSE detector:* An improved version of the detector based on Volterra model has been proposed in [19]. At the receiver, a sufficient statistic is extracted by using oversampling. A fractionally-spaced minimum mean-square error (FS-MMSE) equalizer, working at twice the symbol rate, then acts as an adaptive filter, followed by a BCJR algorithm. With respect to the previous detectors, now we do not rely on any specific signal model and the detector is completely blind.

We finally point out that the chip detector and the FS-MMSE detector can be also used jointly with a predistorter at the transmitter, such as that proposed [20] and also investigated in [11]. In this case, when memory  $L = 0$  is assumed, the FS-MMSE detector becomes equivalent to the *Enhanced Receiver* of [3], the only difference being that the filter is fully adaptive.

#### V. ITERATIVE DETECTION AND DECODING

Common DVB-S2 receivers usually perform detection and decoding separately, with a pragmatic approach. However, it is well known that performing iterative detection and decoding at the receiver improves the performance with a limited complexity increase. Moreover, DVB-S2 standard foresees the use of the low density parity check (LDPC) codes specified in [1], with blocklength 16200 or 64800 bits. These codes have low rate granularity, which does not allow to work at all the spectral efficiency values of interest nowadays.

For these reasons, we have also analyzed the performance with iterative detection and decoding and with the new LDPC codes introduced in DVB-S2X [2], which allow having finer granularity, and, hence, are expected to provide better performance with respect to those foreseen by DVB-S2 when specific SNR targets are to be met.

#### VI. TRANSMIT OPTIMIZATION TECHNIQUES

The aim of this section is to present some possible techniques to improve SE that can be applied at the transmitter. Our aim is to suitably optimize the baudrate, the constellations, and the shaping pulse  $p(t)$ .

##### A. Baudrate Optimization: Time Packing

In satellite systems, orthogonal signaling (i.e.,  $\tau = 1$ ) is often adopted to avoid ISI, at least in the absence of nonlinear distortions. When finite-order constellations are considered (e.g., phase-shift keying (PSK)), it is known that the SE can be improved by relaxing the orthogonality condition ( $\tau < 1$ ). In this case, we are working in the domain of the *Faster-than-Nyquist* paradigm [4]–[7] or its extension known as *time packing* [8]–[10].

The properties of ASE in (1) as a function of  $\tau$  cannot be determined in closed form, but it is clear, by physical

arguments, that it is bounded, continuous in  $\tau$ , and tends to zero when  $\tau \rightarrow 0$  or  $\tau \rightarrow \infty$ . Hence, ASE has a maximum value, when varying  $\tau$ . The optimization problem consists of finding the value of  $\tau$  that results in the maximum ASE; this problem can be studied by evaluating (1) performing a coarse search on the values of  $\tau$ .

### B. Constellation and Shaping Pulse Optimization

As far as the constellation is concerned, the optimization algorithm that allowed to obtain the best performance is a variant of the classical Gradient Descent (GD) algorithm, which has been used to solve the following optimization problem

$$\mathcal{C}^* = \arg \max_{\mathcal{C}: |\mathcal{C}|=M} I_R(\mathcal{C}),$$

in which we have explicitly pointed out the dependence of the information rate  $I_R$  on the constellation.

The steps of the GD algorithm can be summarized as follows.

- 1) Choose randomly  $M$  points in the complex plane, with the only constraint that they must form an energy-normalized constellation called  $\mathcal{C}_0$ . Then set  $\mathcal{C}^* = \mathcal{C}_0$  and compute  $I_R^* = I_R(\mathcal{C}_0)$ .
- 2) At each iteration  $\ell = 1, 2, \dots$  of the GD algorithm, choose randomly one of the  $M$  points of  $\mathcal{C}_{\ell-1}$  and move it to an adjacent free point (where adjacent means on an adjacent vertex of a square grid whose steps are equal to the step size of the GD) to form the new constellation  $\mathcal{C}_\ell$ ; then normalize  $\mathcal{C}_\ell$ .
- 3) Compute  $I_R(\mathcal{C}_\ell)$ . If  $I_R(\mathcal{C}_\ell) > I_R^*$ , set  $I_R^* = I_R(\mathcal{C}_\ell)$  and  $\mathcal{C}^* = \mathcal{C}_\ell$ , otherwise set  $\mathcal{C}_\ell = \mathcal{C}_{\ell-1}$ . Go to step 2.

Since the exact shape of the function  $I_R(\mathcal{C})$  is unknown for the case of interest, to avoid the problem of the optimization process possibly being trapped in some local maximum, we performed the optimization by running several parallel instances of the GD algorithm, each starting from a different random constellation. We then chose the best solution, in terms of information rate, among all instances. In this way, our procedure becomes a *Multistart* Gradient Descent algorithm.

The optimization of the constellation is a complex procedure, requiring a great amount of memory and thousands of iterations to converge to a good solution. To keep the complexity manageable, we used the FS-MMSE detector rather than the chip detector, since our aim at this stage was to find the best constellation. The optimized constellations can then be used with every kind of detector.

We have then attempted a further optimization by applying a similar procedure to the shaping pulse  $p(t)$ : we have considered the information rate  $I_R$  as a function of  $p(t)$ , and we have applied the GD algorithm to each sample of the pulse. However, the high number of samples of a pulse makes the computation unfeasible for values of  $M > 4$ , and even with a QPSK the operation is very slow and there is no guarantee that it will converge to a good solution. Our attempts to optimize the pulse did not bring any advantage to the spectral efficiency of the system. We have also tried to use different kinds of

pulses, like raised cosine or Gaussian pulses, but they showed no gain with respect to the classical RRC pulse.

To conclude the analysis of optimization techniques, we point out that we have also attempted joint optimization of the constellations/shaping pulses in the presence of time packing. However, due to the high complexity of this joint optimization problem, we have been able to obtain only partial results, whose advantages are too limited to be of any interest. As an example to give an insight on the complexity of the problem, we can mention that the optimized pulses result to be very sensitive to the memory  $L$  and to the time packing factor  $\tau$ . This means that an optimized pulse for some values of  $L$  and  $\tau$  can be highly suboptimal for other values. Hence, a good pulse optimization should be performed for several values of  $L$  and  $\tau$ , and for different constellations, but this has not been possible due to the high complexity of the problem.

## VII. NUMERICAL RESULTS

We now show the numerical results for the modulation formats foreseen by the DVB-S2 standard, i.e., PSK and amplitude/phase shift keying (APSK) with their relative bit mapping [1]; as already explained, we have used RRC-shaped  $p(t)$  with roll-off  $\alpha = 0.1$  and bandwidth  $W = 40.7$  MHz. The input back-off (IBO) has been chosen to optimize the performance for each analyzed scenario.

Figs. 2 and 3 show the ASE computed for the three considered detectors with 8PSK and 16APSK, when  $\tau = 1$  is adopted, corresponding to a baudrate of 37 Mbaud. The IBO has been optimized to 0 dB for 8PSK, and to 3 dB for 16APSK. Predistortion has been applied to 16APSK, except for the SISO Volterra detector, which has been designed to work without a predistorter. SISO Volterra and FS-MMSE detectors are working on a symbol-by-symbol base ( $L = 0$ ) since we found that higher memory values do not improve ASE significantly. On the other hand, the chip detector has been tested with increasing values of memory  $L$  until the ASE saturation is reached (i.e., when two consecutive values of  $L$  result in the same ASE). Results show that the lower complexity detectors are practically equivalent and they both reach almost optimal performance. In light of these results, it is worth to point out that the adoption of a properly designed symbol-by-symbol detector is almost optimal, and more sophisticated algorithms cannot provide any performance improvement, independently of the signal model considered at the detector.

We remind the reader that the ASE is achievable by receivers performing iterative detection and decoding. However, if iterations are not allowed, a loss is likely to occur. To evaluate this loss, we report in Fig. 4 the comparison between ASE and p-ASE for FS-MMSE detector with QPSK, 8PSK, and 16APSK. The distance of approximately  $0.2 \div 0.3$  dB between the ASE and p-ASE curves for 16APSK means that there is room for an improvement when allowing iterations between detector and decoder. On the other hand, no improvement is expected for QPSK and 8PSK. This is not surprising, since

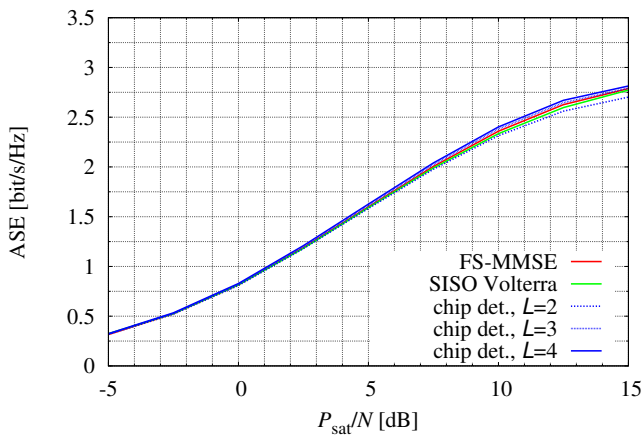


Figure 2. ASE for 8PSK modulation with orthogonal signaling.

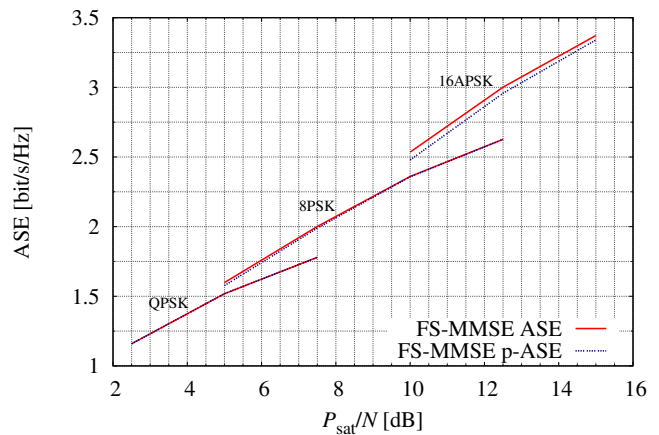


Figure 4. ASE and p-ASE curves for QPSK (IBO=0 dB), 8PSK (IBO=0 dB), and 16APSK (IBO=3 dB) modulations.

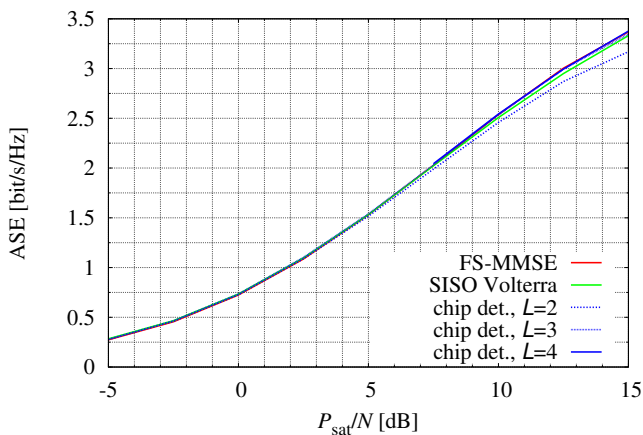


Figure 3. ASE for 16APSK modulation with orthogonal signaling.

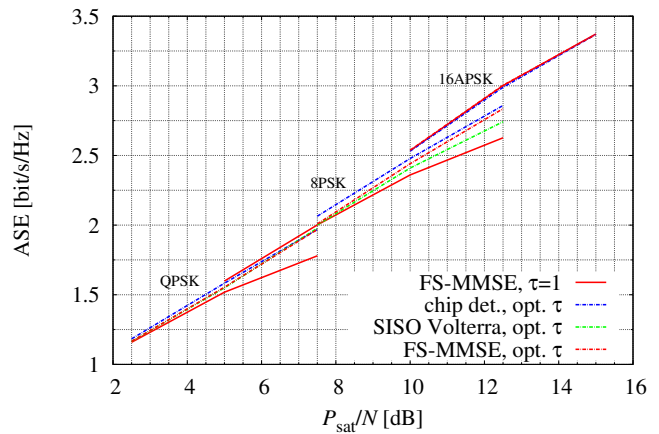


Figure 5. ASE for all described detectors when time packing is employed.

QPSK and 8PSK use a Gray mapping, and thus no gain has to be expected when performing iterations with the detector [21].

After this analysis, which shows that improving the detector alone cannot give spectral efficiency gains, we have proceeded to the application of the transmit optimization techniques described in Section VI.

Fig. 5 depicts ASE computed with optimized values of  $\tau$  for the three considered detectors and for the three modulation formats of interest. The considered memory for all detection algorithms is  $L = 5$  in case of QPSK and 8PSK, and  $L = 4$  in case of 16APSK. From this figure, it can be seen that for QPSK the three detection schemes are quite equivalent, and time packing provides a gain in terms of ASE of approximately 14% at  $P_{\text{sat}}/N = 7.5$  dB w.r.t. orthogonal signaling. It is worth mentioning that considering this result alone is misleading: at the selected  $P_{\text{sat}}/N$  value, QPSK is no longer the optimal constellation, and by moving to 8PSK this gain disappears. In case of 8PSK, the chip detector exhibits a gain of approximately 5% at  $P_{\text{sat}}/N = 10$  dB and it slightly outperforms the other

two detectors. However the same conclusions as for QPSK apply, since 16APSK outperforms 8PSK at this  $P_{\text{sat}}/N$  value. Finally, for 16APSK modulation, time packing is unable to provide any gain.

Fig. 6 compares the envelope of chip detector ASE curves in Figure 5 with orthogonal signaling. This figure shows that the potential of time packing on the satellite channel is very limited. In fact, for medium-high  $P_{\text{sat}}/N$  values, 16APSK with  $\tau = 1$  outperforms time packing. We can conclude that benefits of time packing are too limited, and only at low  $P_{\text{sat}}/N$ , to justify the complexity increase necessary to apply this technique. For these reasons, we will not further deal with time packing in the rest of the paper. However, the reader has to consider that, in practice, a sort of surrogate of time packing has already been introduced with the optimization of the  $W$ . In fact, by increasing the value of  $W$  we increase ISI due to the fact that the bandwidth of IMUX and OMUX filters are kept fixed, as in the case of time packing [10].

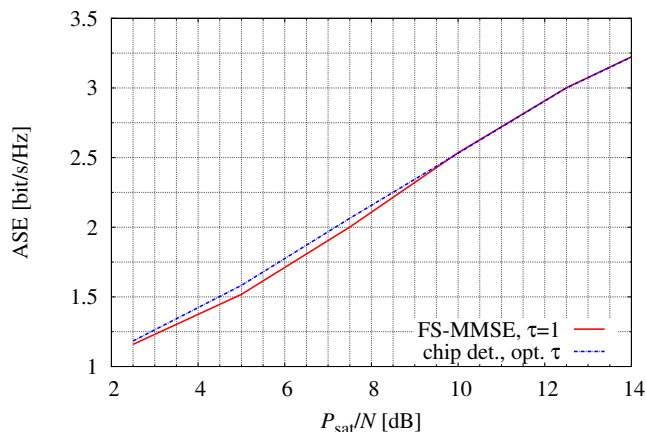


Figure 6. ASE envelope in case of optimized time packing and the chip detector.

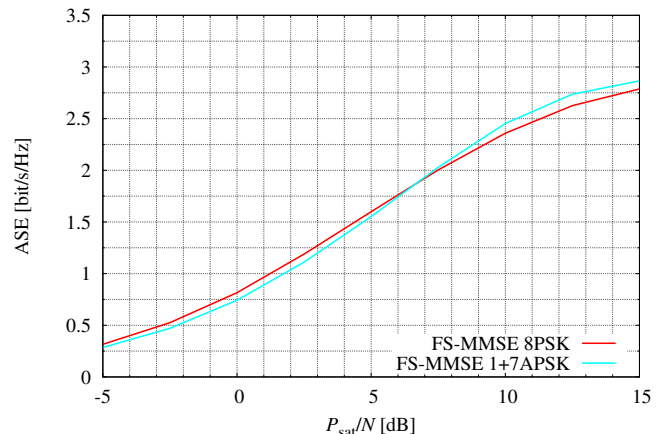


Figure 7. ASE comparison for 8PSK (IBO=0 dB) and 1+7APSK (IBO=3 dB) with FS-MMSE detector.

We then investigated the application of the constellation optimization algorithm described in Section VI-B to the cases of  $M = 4, 8, 16$ , and we obtained the following results (independently of the IBO).

- 1) In the case  $M = 4$ , the optimal constellations converged almost perfectly to a classical QPSK.
- 2) In the case  $M = 8$ , the optimized constellations resulted to be 8PSK at low  $P_{\text{sat}}/N$  and a 1+7APSK at high  $P_{\text{sat}}/N$ , being 1+7APSK composed of a point in the origin of the complex plane and seven point equally spaced on a circle. This behavior is clear from Figure 7, that plots the ASE for the two modulation formats for their best IBO.
- 3) In the case  $M = 16$ , the algorithm converged to 3+13APSK for the  $P_{\text{sat}}/N$  values of interest.<sup>1</sup> However, when the signal is predistorted, we found that classical 16APSK provides the best results, thus there is no need to replace that constellation.

In order to confirm the information theoretic analysis, we simulated the PER of MODCODs employing the DVB-S2 LDPC codes with blocklength 64800 bits [1] and the LDPC codes with the same length, introduced in DVB-S2X [2].

In Fig. 8 we evaluated the PER for 8PSK and 1+7APSK, using the DVB-S2X codes with rates  $r$  equal to 11/20, 104/180, 18/30, and 20/30 foreseen by [2]. We can see that these results confirm the theoretical curves shown in Figure 7, with 1+7APSK that tends to outperform 8PSK for  $P_{\text{sat}}/N$  greater than about 6.5 dB.

Finally, we summarized the practical MODCODs we found in Fig. 9, where the arrows point to the first MODCOD using the corresponding modulation format (for each curve, the points before the arrow are obtained with QPSK). We

<sup>1</sup>It is interesting to notice that the number of points of the inner circle tends to increase with  $P_{\text{sat}}/N$ , as already pointed out in [22] for different scenarios. However these  $P_{\text{sat}}/N$  values are not of interest for the problem we are considering.

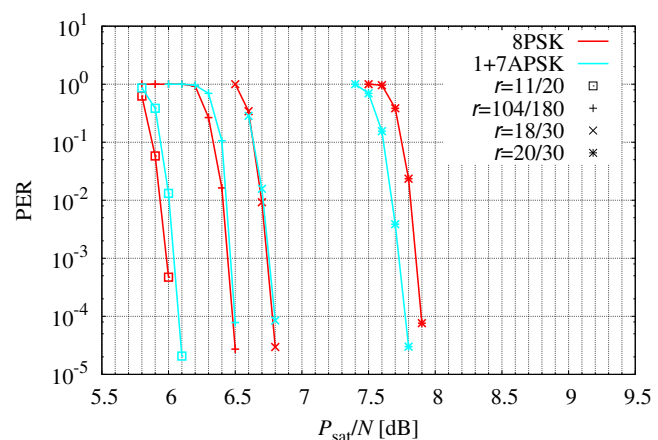


Figure 8. PER for DVB-S2X codes, with 8PSK and 1+7APSK, with FS-MMSE detector and iterative detection and decoding.

reported in red the spectral efficiency for MODCODs with DVB-S2 codes. We see that performing iterations between detector and decoder (continuous line) allows about 0.2 dB gain w.r.t. the absence of iterations (dashed line) for 16APSK only. We simulated DVB-S2X codes (blue line) and we see that they always gain w.r.t. DVB-S2. The gains are due in part to an improvement in the code design, but mainly due to the higher granularity that allows to better cover the spectral efficiency plane, especially the  $P_{\text{sat}}/N$  regions corresponding to modulation changes (e.g., 9 ÷ 11 dB). To conclude the analysis, we show that, for some MODCODs, the adoption of 1+7APSK allows a further gain of about 0.1 ÷ 0.2 dB.

## VIII. CONCLUSIONS

We have addressed the problem of improving the spectral efficiency of DVB-S2X systems through advanced techniques. We have considered, as our starting point, a DVB-S2 system with optimized baudrate and roll-off, adopting, at the receiver, an equalizer followed by a symbol-by-symbol detector. In this

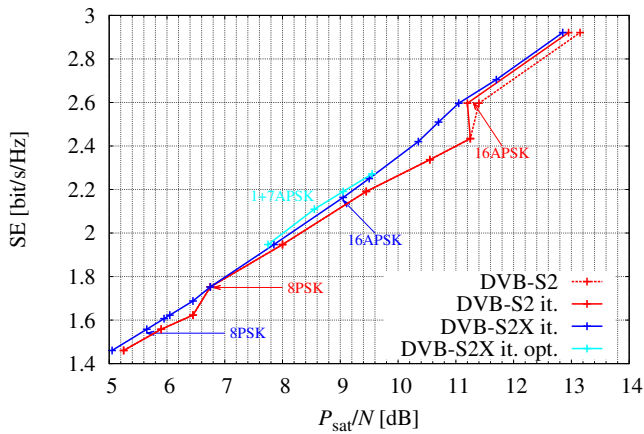


Figure 9. Practical MODCODs.

scenario, it is unfeasible to further increase the bandwidth of signals, hence advantages must be researched in different ways.

First of all, we have studied the application of more sophisticated detection techniques, showing that improving the detector alone cannot give significant advantages; from this observation, we could conclude that a properly designed symbol-by-symbol detector is practically optimal in the scenarios of interest.

After pointing out the advantages of performing iterative detection and decoding, and introducing the new improved DVB-S2X LDPC codes, we moved to study transmit optimization techniques, such as time packing and constellation and/or shaping pulse optimization. While time packing could not guarantee any performance improvement in the regions of interest, we found that a properly designed constellation could give (limited) advantages in some cases of interest.

We have evaluated both theoretical performance, in terms of achievable spectral efficiency, and the spectral efficiency of practical modulation and coding formats showing a strong agreement between them.

#### ACKNOWLEDGMENTS

This work is funded by RAI, Research and Technology Innovation Centre, Torino, Italy.

#### REFERENCES

- [1] ETSI EN 301 307 Digital Video Broadcasting (DVB); V1.1.2 (2006-06), Second generation framing structure, channel coding and modulation systems for Broadcasting, Interactive Services, News Gathering and other Broadband satellite applications, 2006, Available on ETSI web site (<http://www.etsi.org>).
- [2] Digital Video Broadcasting (DVB), DVB Document A83-2, Second generation framing structure, channel coding and modulation systems for Broadcasting, Interactive Services, News Gathering and other Broadband satellite application, Part II: S2-Extensions (DVB-S2X), Mar. 2014.
- [3] S. Cioni, G. Colavolpe, C. Ernst, and A. Ginesi, "Bandwidth Optimization for Satellite Digital Broadcasting," in *31st AIAA International Communications Satellite Systems Conference*, Florence, Italy, Oct. 2013.
- [4] J. E. Mazo, "Faster-than-Nyquist signaling," *Bell System Tech. J.*, vol. 54, pp. 1450–1462, Oct. 1975.

- [5] J. E. Mazo and H. J. Landau, "On the minimum distance problem for faster-than-Nyquist signaling," *IEEE Trans. Inform. Theory*, pp. 1420–1427, Nov. 1988.
- [6] A. Liveris and C. N. Georghiades, "Exploiting faster-than-Nyquist signaling," *IEEE Trans. Commun.*, vol. 47, pp. 1502–1511, Sep. 2003.
- [7] F. Rusek and J. B. Anderson, "The two dimensional Mazo limit," in *Proc. IEEE International Symposium on Information Theory*, Adelaide, Australia, Nov. 2005, pp. 970–974.
- [8] A. Barbieri, D. Fertonani, and G. Colavolpe, "Time-frequency packing for linear modulations: spectral efficiency and practical detection schemes," *IEEE Trans. Commun.*, vol. 57, pp. 2951–2959, Oct. 2009.
- [9] A. Modenini, G. Colavolpe, and N. Alagha, "How to significantly improve the spectral efficiency of linear modulations through time-frequency packing and advanced processing," in *Proc. IEEE Intern. Conf. Commun.*, Ottawa, Canada, Jun. 2012, pp. 3299–3304.
- [10] A. Piemontese, A. Modenini, G. Colavolpe, and N. Alagha, "Improving the spectral efficiency of nonlinear satellite systems through time-frequency packing and advanced processing," *IEEE Trans. Commun.*, vol. 61, no. 8, pp. 3404–3412, Aug. 2013.
- [11] E. Casini, R. De Gaudenzi, and A. Ginesi, "DVB-S2 modem algorithms design and performance over typical satellite channels," *Intern. J. of Satellite Communications and Networking*, vol. 22, no. 3, pp. 281–318, May/June 2004.
- [12] D. M. Arnold, H.-A. Loeliger, P. O. Vontobel, A. Kavčić, and W. Zeng, "Simulation-based computation of information rates for channels with memory," *IEEE Trans. Inform. Theory*, vol. 52, no. 8, pp. 3498–3508, Aug. 2006.
- [13] N. Merhav, G. Kaplan, A. Lapidoth, and S. Shamai, "On information rates for mismatched decoders," *IEEE Trans. Inform. Theory*, vol. 40, no. 6, pp. 1953–1967, Nov. 1994.
- [14] J. B. Soriaga, H. Pfister, and P. Siegel, "Determining and approaching achievable rates of binary intersymbol interference channels using multistage decoding," *IEEE Trans. Inform. Theory*, vol. 53, pp. 1416–1429, Apr. 2007.
- [15] S. Benedetto, E. Biglieri, and V. Castellani, *Digital Transmission Theory*. Englewood Cliffs, NJ: Prentice-Hall, 1987.
- [16] L. R. Bahl, J. Cocke, F. Jelinek, and J. Raviv, "Optimal decoding of linear codes for minimizing symbol error rate," *IEEE Trans. Inform. Theory*, vol. 20, pp. 284–287, Mar. 1974.
- [17] G. Colavolpe, A. Modenini, and F. Rusek, "Channel shortening for nonlinear satellite channels," *IEEE Commun. Letters*, vol. 16, pp. 1929–1932, Dec. 2012.
- [18] G. Colavolpe and A. Piemontese, "Novel SISO detection algorithms for nonlinear satellite channels," *IEEE Wireless Commun. Letters*, vol. 1, no. 1, pp. 22–25, Feb. 2012.
- [19] A. Modenini, "Advanced transceivers for spectrally-efficient communications," Ph.D. dissertation, University of Parma, Parma, Italy, Jan. 2014.
- [20] G. Karam and H. Sari, "Analysis of predistortion, equalization, and ISI cancellation techniques in digital radio systems with nonlinear transmit amplifiers," *IEEE Trans. Commun.*, vol. 37, pp. 1245–1253, Dec 1989.
- [21] S. ten Brink, "Designing iterative decoding schemes with the extrinsic information transfer chart," *AEU Int. J. Electronic. Commun.*, vol. 54, no. 6, pp. 389–398, Dec. 2000.
- [22] F. Kayhan and G. Montorsi, "Constellation design for transmission over nonlinear satellite channels," in *Proc. IEEE Global Telecommun. Conf.*, Anaheim, CA, U.S.A., Dec. 2012, pp. 3401–3406.